Received: 20 May 2019 | Accepted: 11 October 2019

DOI: 10.1111/pce.13665

ORIGINAL ARTICLE

WILEY Plant, Cell & Environment

Day length regulates seasonal patterns of stomatal conductance in *Quercus* species

Elena Granda[1,2] | Frederik Baumgarten[3] | Arthur Gessler[3] | Eustaquio Gil-Pelegrin[4] | Jose Javier Peguero-Pina[4] | Domingo Sancho-Knapik[4] | Niklaus E. Zimmermann[3] | Víctor Resco de Dios[5,1]

[1] Department of Crop and Forest Sciences—AGROTECNIO Center, Universitat de Lleida, Lleida 25198, Spain

[2] Department of Life Sciences, University of Alcalá, Alcalá de Henares E-28805, Spain

[3] Forest Dynamics, Swiss Federal Institute for Forest, Snow and Landscape Research WSL, Zürcherstrasse 111, Birmensdorf CH-8903, Switzerland

[4] Unidad de Recursos Forestales, Centro de Investigación y Tecnología Agroalimentaria de Aragón, Gobierno de Aragón, Avda. Montañana 930, Zaragoza 50059, Spain

[5] School of Life Science and Engineering, Southwest University of Science and Technology, Mianyang 621010, China

Correspondence
E. Granda, Department of Crop and Forest Science—AGROTECNIO Center, Universitat de Lleida, Av. Rovira Roure 191, Lleida 25198, Spain.
Email: elena.granda.f@gmail.com
V. Resco de Dios, School of Life Science and Engineering, Southwest University of Science and Technology, Mianyang 621010, China.
Email: vic@pvcf.udl.cat

Funding information
Southwest University of Science and Technology, Grant/Award Number: 18ZX7131; Velux Foundation, Switzerland, Grant/Award Number: 1119; PHOTOCHAIN

Abstract

Vapour pressure deficit is a major driver of seasonal changes in transpiration, but photoperiod also modulates leaf responses. Climate warming might enhance transpiration by increasing atmospheric water demand and the length of the growing season, but photoperiod-sensitive species could show dampened responses. Here, we document that day length is a significant driver of the seasonal variation in stomatal conductance. We performed weekly gas exchange measurements across a common garden experiment with 12 oak species from contrasting geographical origins, and we observed that the influence of day length was of similar strength to that of vapour pressure deficit in driving the seasonal pattern. We then examined the generality of our findings by incorporating day-length regulation into well-known stomatal models. For both angiosperm and gymnosperm species, the models improved significantly when adding day-length dependences. Photoperiod control over stomatal conductance could play a large yet underexplored role on the plant and ecosystem water balances.

KEYWORDS

circadian rhythm, day length, gas exchange, latitude, Mediterranean, *Quercus*, stomatal control, temperate, tropical, woody plants

1 | INTRODUCTION

Global warming is leading to longer growing seasons and higher atmospheric water demand, which exerts a significant impact over the water cycle and transpirational water losses. The effects of seasonal warming on transpiration are mediated by leaf level stomatal conductance. Photoperiod is a major driver of leaf phenology, but a potential role for photoperiod responses as modulators of seasonal stomatal behaviour has not been properly evaluated.

The interplay between temperature and photoperiod (i.e., day length) affects phenological processes such as flowering time, budburst, seasonal stem growth, leaf senescence, and dormancy (Basler & Körner, 2012; Jackson, 2009; Luo et al., 2018; Rossi et al., 2006; Tylewicz et al., 2018; Way & Montgomery, 2015; Zohner, Benito, Svenning, & Renner, 2016; Zohner & Renner, 2015). Day length has also been documented to be a driver of seasonal changes in the photosynthetic capacity of leaves and ecosystems at similar or

even larger importance as temperature (Bauerle et al., 2012; Bongers, Olmo, Lopez-Iglesias, Anten, & Villar, 2017; Stinziano & Way, 2017; Stoy, Trowbridge, & Bauerle, 2014; Way, Stinziano, Berghoff, & Oren, 2017). Circumstantial evidence points towards a potentially important day-length effect also on stomatal conductance. Zhao, Li, Duan, Korpelainen, and Li (2009), for example, observed how both photosynthesis and stomatal conductance declined in *Populus cathayana* under short-day photoperiods. However, the decline was much more marked in conductance (~50% decline) than in photosynthesis (~30% decline) for male poplars. This is in line with the control of gas exchange by the circadian clock that underlies all photoperiod-responsive processes as the effects of circadian regulation are more important over stomatal conductance than over photosynthesis (Resco de Dios & Gessler, 2018). The current view on intra-annual variation in stomatal conductance is that it is driven by the interplay between environmental drivers (e.g., soil moisture and vapour pressure deficit), but the role of day length remains unexplored.

The effects of day length on leaf physiology are thought to vary depending on the latitudinal origin of a species (Becklin et al., 2016), although it is unclear whether day length effects increase or decrease with latitude. The traditional view is that the seasonality in insolation and day length increases with latitude and, consequently, photoperiod at higher latitudes should provide a stronger signal than at lower latitudes (Saikkonen et al., 2012) in order to protect leaves and other tissues against, for instance, late frosts in the spring or other environmental stresses. Conversely, the study of Zohner et al. (2016) found, within the temperate biome, that species relying on photoperiod as a budburst signal were more commonly found at lower latitudes with shorter winters, whereas photoperiod-sensitive budburst was rare at higher latitudes. Consequently, the understanding of how the geographical origin determines the degree of photoperiod sensitivity is unresolved.

In the present study, we tested the general hypothesis that seasonal changes in stomatal conductance are driven not only by temperature or air-to-leaf vapour pressure deficit when soil water is not restricting but also by changes in day length. First, we measured gas exchange weekly over a growing season in 12 *Quercus* species whose natural distribution ranged from tropical (~8°N) to temperate latitudes (~60°N), although no single species spanned the whole latitudinal range. We used different types of statistical as well as semi-mechanistic stomatal models to quantify the potential importance of day length and test the hypotheses that (a) day length is a significant driver of seasonal variation in stomatal conductance; (b) the effect of day length is of similar magnitude to that of temperature or *VPD* over seasonal scales; and (c) the dependence on day length would vary with the natural distribution range of a species. We selected oaks for our study because they are common or dominant trees species across a wide variety of habitats and biomes (Gil-Pelegrín, Peguero-Pina, & Sancho-Knapik, 2017).

Second, after demonstrating significant effects of day length over 12 *Quercus* species, we aimed at testing whether our results would also apply to a broader selection of species. Consequently, we searched for additional datasets on stomatal conductance publicly available (Anderegg et al., 2018; Lin et al., 2015) and tested whether adding a photoperiod component in a commonly used stomatal model (Medlyn et al., 2011) improved predictions of seasonal stomatal conductance in additional tree species distributed across the globe for which data are currently available. Here, we demonstrate, for the first time to our knowledge, that photoperiod exerts a major control on the seasonal pattern of stomatal conductance.

2 | METHODS

2.1 | Study species and experimental site

A total of 12 *Quercus* species from different geographical origins (TEM, temperate; MED, Mediterranean; and TRO, tropical) were selected in order to represent a wide latitudinal spectrum, ranging from 8°N in Panamá to 60°N in southern Sweden (Table S1). Four species per origin (TEM: *Quercus robur*, *Quercus rubra*, *Quercus macrocarpa*, and *Quercus variabilis*; MED: *Quercus ilex* subsp. *ilex*, *Quercus faginea*, *Quercus ilex* subsp. *ballota*, and *Quercus douglassi*; and TRO: *Quercus acutifolia*, *Quercus lanata*, *Quercus myrsinifolia*, and *Quercus semecarpifolia*) and four saplings per species were used for this experiment (n = 48). Saplings had the same age within species (between 5 and 10 years old among species), with mean (±SE) height of 75 ± 4 cm and trunk diameter measured at 10 cm from the ground of 1.2 ± 0.1 cm. In spring 2018, plants were located outdoors at the Forest Research Unit, CITA de Aragón (41.39°N, 0.52°W, Zaragoza, Spain) under uniform light conditions, and they were watered daily to field capacity to avoid drought stress. Pots with 30-cm depth and 20-L capacity were filled with a mixture of 80% compost (Neuhaus Humin Substrat N6; Klasman-Deilmann GmbH, Geeste, Germany) and 20% perlite. Nutrients were supplied as slow-release fertilizer (Osmocote Plus, Sierra Chemical, Milpitas, CA, USA). The fertilizer (3 g L^{-1} of soil) was applied to the top 10-cm layer of substrate. All plants were grown under the same environmental conditions. Air temperature (T, °C) and relative humidity (RH, %) were measured every hour at the experimental site using a Hobo Pro temp/RH data logger (Onset Computer, Bourne, MA, USA) located at 1.30 m above the soil surface and right above the saplings canopy. Hourly net radiation (W m^{-2}) and precipitation (mm) were provided by the Aragón Government from a nearby station (Montañana, Oficina del Regante, Figure 1).

2.2 | Physiological measurements

We originally intended to collect measurements from the spring to the autumn equinoxes in 2018; however, experiment inception had to be delayed due to leaf phenology. That is, we could not start our weekly measurements until May 29, when leaves were fully developed (especially for evergreen species, which needed longer periods to terminate leaf development), and measurements lasted until October 25. They were conducted in fully expanded, sun-exposed leaves over a short window of time (10:30 a.m. to 1:30 p.m.) to minimize circadian effects and during 2 days (consecutive whenever possible) per week. Stomatal

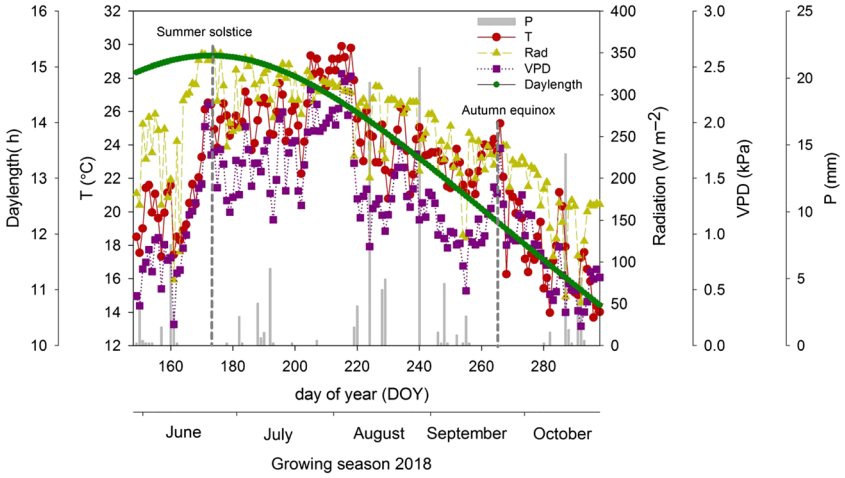

FIGURE 1 Mean daily meteorological conditions of temperature (°C), radiation (W m^{-2}), *VPD* (kPa), daily precipitation (*P*, mm) and day length (hr) from the end of May until the end of October of 2018 in the study site located in Zaragoza, Spain

conductance to water vapour (g_s) was measured using a CIRAS-2 portable photosynthesis system (PP Systems, Amesbury, MA, USA) fitted with an automatic universal leaf cuvette (PLC6-U, PP Systems). Radiation was set at a saturating photosynthetic photon flux density of 1,500 μmol m^{-2} s^{-1}. The controlled cuvette CO_2 concentration (C_a = 400 μmol mol^{-1}) was maintained using an automatic control device on the CIRAS-2, whereas the relative humidity (*RH*) and block temperature mirrored that of the environment.

2.3 | Statistical analyses

We first tested for a statistically significant pattern of seasonal variation in stomatal conductance. We modelled the temporal patterns in g_s, after grouping species by their geographical origin (TEM, MED, and TRO), using generalized additive models (GAMs, Hastie & Tibshirani, 1990). GAMs are a nonparametric extension of generalized linear models (GLMs) in which we fitted smooth curves to data using local smoothing functions instead of the parametric functions as in GLMs. One of the main strengths of GAMs is that they do not assume any predetermined functional relationship between dependent and independent variables. We then tested whether the temporal pattern was statistically significant by analysing the first derivative (the slope or rate of change) with the finite differences method. We also computed standard errors and a 95% pointwise confidence interval for the first derivative. The trend was subsequently deemed significant when the derivative confidence interval was bounded away from zero at the 95% level (for full details on this method, see Curtis & Simpson, 2014). Periods with significant variation are illustrated on the figures by the yellow line portions, and nonsignificant differences occur elsewhere.

After testing for statistical variation in the seasonal pattern, we sought to test which environmental factors were explaining the temporal pattern. First, we explored the relationships between our dependent variable (g_s) and the environmental drivers (*VPD*, *T*, radiation, and day length) from the cuvette, which mimicked the environmental conditions at the time of measurement, through simple linear models, transforming variables where necessary to achieve normality. For *VPD* and radiation, non-linear, exponential fits were computed with the nls method (Bates & Watts, 1988), and to determine the goodness of the fit, we computed the residual sum of squares (lack of fit) and the complement of its proportion to the total sum of squares (coefficient of determination, R^2 = 1 − (RSS/TSS).

To more rigorously test for statistical relationships, we applied linear mixed-effects models, using tree species and week of measurement as random factors. The fixed factors in the linear mixed models were day length, radiation, *VPD*, and their interaction with the geographical origin to test for potential differences across biomes. The best fixed and random structures of the model were tested using the Akaike information criterion (AIC, Burnham & Anderson, 2002). The initial linear models were simplified using dredging techniques based on AIC to obtain the optimal model (Barton, 2018). Some of our *Quercus* species were evergreen, and others were deciduous. We thus also included leaf type (evergreen or deciduous) as a fixed effect instead of the origin of the species in our models (results not shown), but leaf type was never included in the best model, indicating that the responses did not depend on this trait. Models were implemented using the "nlme" (Pinheiro, Bates, DebRoy, & Sarkar, 2018), "MuMIn" (Barton, 2018), and "mgcv" (Wood, 2017) R packages from Version 3.5 (R Core Team, 2018). We also calculated the per cent of variation explained by the mixed models following Nakagawa and Schielzeth (2013).

2.4 | Stomatal conductance models

To further assess the importance of day length as a regulator of seasonal variation in stomatal conductance, and to improve our understanding of the generality of our results, we modified a commonly used model of stomatal conductance to incorporate day-length effects.

First, we fitted our dataset against three models of stomatal conductance that are commonly used in leaf-level simulations and are widely used in Earth system models, namely, the models proposed

by Ball, Woodrow, and Berry (1987), Leuning (1995), and Medlyn et al. (2011). These models are relatively similar, but they differ mostly regarding the representation of the dependence of g_s on atmospheric moisture. For our dataset, we observed that the model of Medlyn et al. (2011) provided the best fit (Table S2). Consequently, we compared the predictions of g_s from the original model of Medlyn et al. (2011):

$$g_s = g_0 + 1.6\left(1 + \frac{g_1}{\sqrt{VPD}}\right)\left(\frac{A}{C_a}\right) \quad (1)$$

against a modified version that incorporates a linear effect of day length affecting the slope component (g_1), such that

$$g_s = g_0 + 1.6\left(1 + \frac{g_1(1 - g_2\, nl)}{\sqrt{VPD}}\right)\left(\frac{A}{C_a}\right), \quad (2)$$

where g_s is the stomatal conductance to water vapour and g_0 and g_1 are fitting parameters related to the minimal conductance to water vapour and the marginal water use efficiency (a concept derived from optimal stomatal theory), respectively. *VPD* is vapour pressure deficit (kPa), *A* is net assimilation rate (μmol m^{-2} s^{-1}), C_a is atmospheric CO_2 concentration at the leaf surface (μmol mol^{-1}), *nl* indicates night length in hours (i.e., 24 minus day length in hours), and g_2 is another fitting parameter.

In this modification of the Medlyn et al. (2011) model, we assume that the effect of day length over g_s is such that increases in night-length linearly decline g_s. We therefore assume that g_s increases linearly through the growing season towards a peak value at the summer solstice and that it then declines again linearly thereafter. This assumption is based on a parsimonious interpretation of the relationship we observed between g_s and photoperiod in our studied oak species (Figure 3b).

The model in Equation (2) further assumes that day length affects the slope parameter of the model (g_1) such that it modulates the effects of the other parameters (*VPD*, *A*, and C_a). However, it is also possible that day length affects the minimal conductance (g_0) or intercept of the model. To test for this possibility, we thus added the day length effect over g_0, also following a linear assumption:

$$g_s = g_0(1 - g_3\, nl) + 1.6\left(1 + \frac{g_1}{\sqrt{VPD}}\right)\left(\frac{A}{C_a}\right), \quad (3)$$

where g_3 is a fitting parameter describing the effect of day length. Finally, we also tested whether day length affected both the slope and the intercept by combining the Equations (2) and (3):

$$g_s = g_0(1 - g_3\, nl) + 1.6\left(1 + \frac{g_1(1 - g_2\, nl)}{\sqrt{VPD}}\right)\left(\frac{A}{C_a}\right). \quad (4)$$

We ran the set of four models in two modelling exercises. First, we randomly chose half of our study species for model calibration, and the remaining half was used for validation (six species in each set). Second, we assessed the generality of our findings by using the data from two recent global-scale databases on g_s (Anderegg et al., 2018; Lin et al., 2015). This dataset provides g_s time series for different species measured under either "ambient" or "control" conditions. That is, this dataset was not restricted to plants in pots, like our previous analyses, and soil water content has thus been varying. From these databases, we selected those studies that measured stomatal conductance in additional tree species at least four times over a period of more than 3 months (i.e., >50% of annual day-length variation). As a result, we were able to incorporate data from 13 additional tree species (Table S3). Additionally, we used one further dataset of our own that measured 5-year-old saplings of *Quercus pubescens* in Birmensdorf, Switzerland, grown in open top chambers. The general set-up of the chamber—lysimeter system—is described by Hagedorn et al. (2016). We fitted the model separately for angiosperms and gymnosperms using Equations (1) and (2) with "nlme" (Pinheiro et al., 2018). We used AIC and the R^2 of the regression of observed versus predicted values as indicators of the goodness of fit of each model.

3 | RESULTS

3.1 | Temporal trends of g_s

We observed significant seasonal variation in g_s across the three groups of oaks. The seasonal maximum occurred around the end of June–mid-July (Figure 2), briefly after the summer solstice (i.e., when the day length is at, or near, its maximum). Significant decreases in g_s (represented by the yellow part of the curve in Figure 2) were found at the end of July for all species.

3.2 | Effects of environmental variables on g_s

When testing single factors alone, we observed that *VPD* and day length were the most important drivers of seasonal g_s in our datasets (Table 1 and Figure 3). Averaged across species, g_s declined from around 200 to 50 mmol m^{-2} s^{-1} as *VPD* varied from 1 to 3.7 kPa and g_s increased from 80 to 200 mmol m^{-2} s^{-1} as day length increased from 10.5 to 15.5 hr (Figure 3a,b) during our measurements. Importantly, we observed that the proportion of variance explained by day length (R^2 = .31) was larger than that explained by *VPD* (R^2 = .24), indicating a potentially important role of day length for process modelling. Relationships of g_s with temperature and radiation were also significant, but the proportion of variation explained by those variables was much smaller (R^2 = .02 and .13, respectively). In fact, radiation was not selected by our stepwise regression approach (see below).

Results from our stepwise linear mixed model selection (R^2 = .53) indicated that g_s was significantly affected by day length (P < .0001), *VPD* (P < .0001), origin (P = .02), and the interaction between day length and origin (P = .006, Table 2). The interaction between the origin of the species (TEM, MED, and TRO) and day length indicated that day length had a stronger positive effect on g_s for MED species,

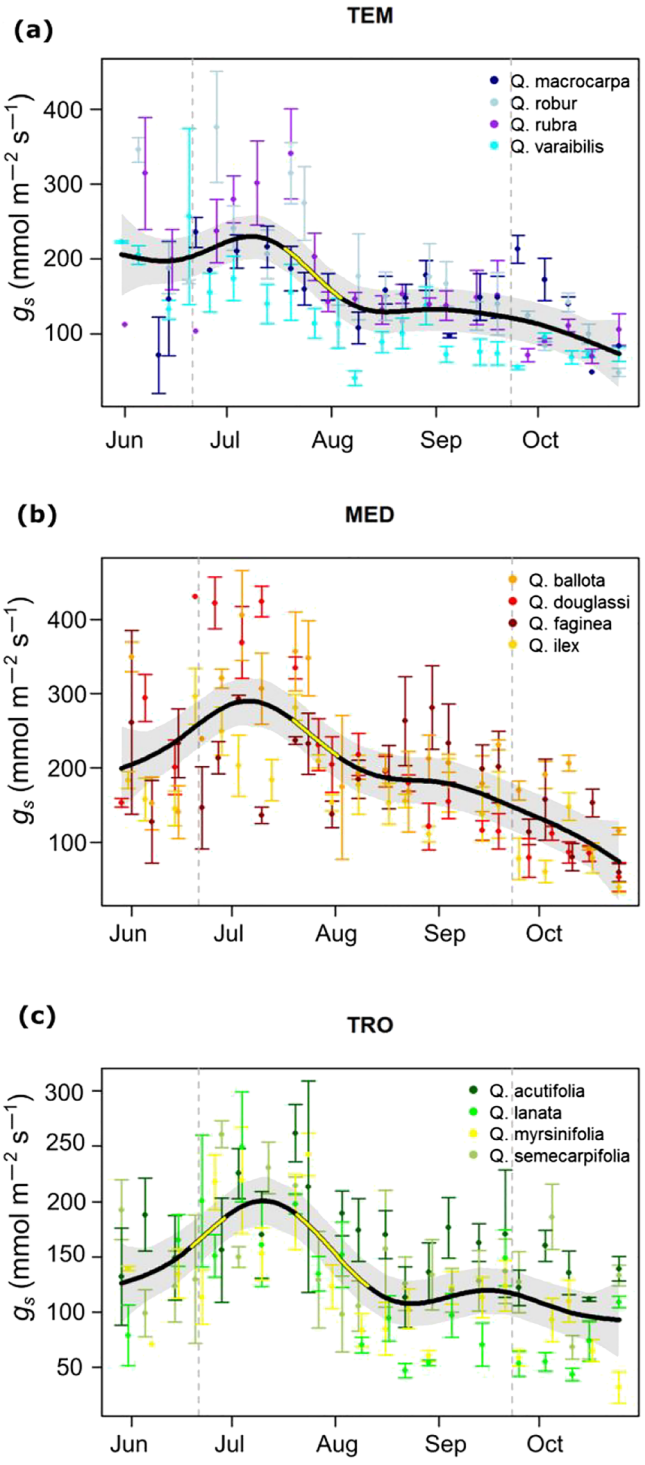

FIGURE 2 Temporal patterns obtained by fitting generalized additive models of (a) the temperate (TEM), (b) Mediterranean (MED), and (c) tropical (TRO) species from the beginning of June until the end of October. The yellow parts of the curve indicate significantly increasing or decreasing slopes. Summer solstice and autumn equinox are indicated by vertical grey lines [Colour figure can be viewed at wileyonlinelibrary.com]

followed by TEM and TRO species that had similar slopes. In other words, the slope of the relationship between g_s and day length was significantly larger for Mediterranean species.

3.3 | Day length in stomatal models

In the first modelling exercise, we used half of our study species (*Q. ballota*, *Q. douglassi*, *Q. lanata*, *Q. macrocarpa*, *Q. myrsinifolia*, and *Q. semecarpifolia*) for calibration and the other half for validation (Tables 3 and S1 and Figure 4). We observed that model fit increased significantly after including day-length effects as the R^2 of the observed versus predicted relationship increased from .36 (in Equation 1, without day-length regulation) to .52–.58 in the models that included day length effects (Equations 2–4). Furthermore, the AIC declined from −368 in the model without photoperiod effects, down to −426 in the model from Equation (3), which included day length as affecting only the minimal conductance (g_0). The R^2 was slightly higher in Equation (2) (which includes day length as affecting only g_1) than in Equation (3) (.58 vs. .53, respectively). However, the AIC was lower in Equation (3) than in Equation (2) (−426 vs. −414), probably because there was a slight bias in the predictions from Equation (2): The slope and intercept of the relationship between observed and predicted values became significantly different from 1 and 0, respectively, in Equation (2) (with day length affecting the slope, Table 3) but not in Equation (3). Summing up, there was a significant increase in model fit after increasing day length regulation, and the most plausible model was that which included day length effects over g_0 (Equation 3).

We examined the changes in model fit after including day length effects in the data available from the literature separately for angiosperms (nine species, Figure 5a,b and Table 3) and for gymnosperms (four species, Figure 5c,d and Table S3). For the angiosperm dataset, we also observed that model fit significantly increased after including day-length effects. The most plausible model was also that in Equation (3), where day-length affects only g_0 (Table 3). The R^2 of the relationship between observed and predicted values increased from .58 in model without day-length effects (Equation 1) up to .63 in Equation (3). This increase in the R^2 was accompanied by a decline in the AIC from −193 in Equation (1) to −199 in Equation (3), indicating that the model from Equation (3) was also more parsimonious.

When examining model performance in conifers, we also observed an increase in model fit after including photoperiod effects (Table 3). However, unlike for angiosperms, here the model that provided the highest R^2 and the lowest AIC was Equation (4), which is the model that assumes that day length regulation modulates both the intercept (g_0) and the slope (g_1) of the model. R^2 increased from .74 in Equation (1) to .79 in Equation (4), and the AIC dropped from −272 to −282.

4 | DISCUSSION

This is the first study, to our knowledge, that documents day length as a significant driver of the seasonal variation in stomatal conductance across a range of woody plants. We observed that the role of day length is of similar importance to that of seasonal variations in vapour

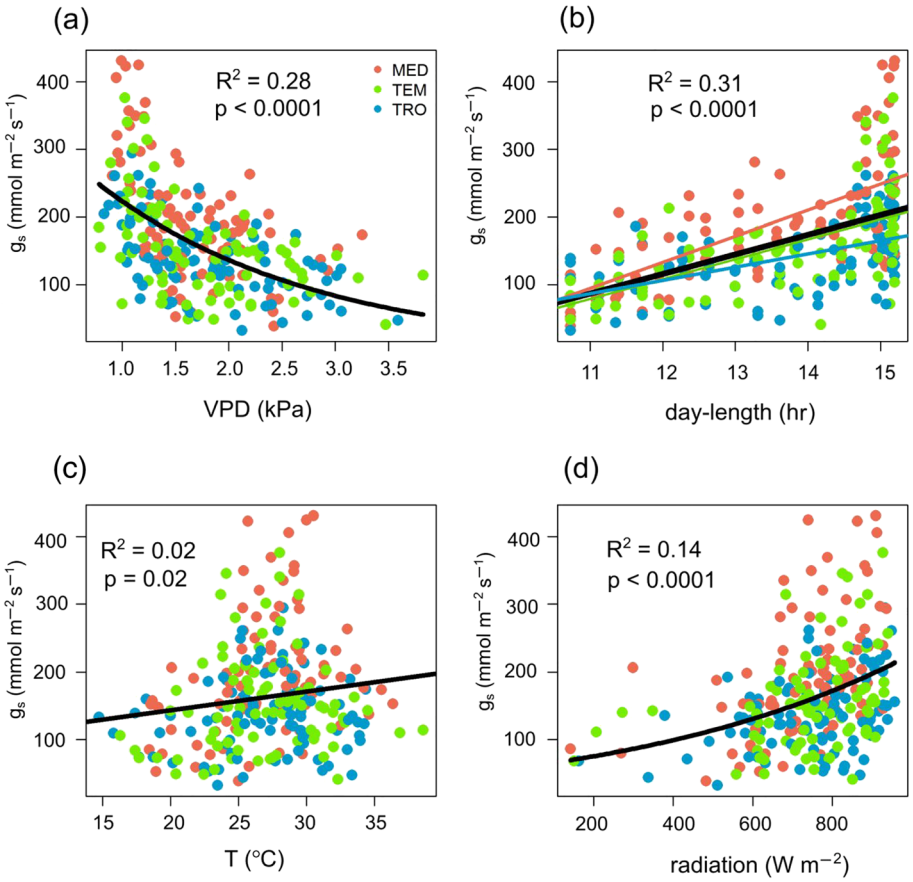

FIGURE 3 Relationship between stomatal conductance (g_s) and four explicative variables: (a) *VPD* (vapour pressure deficit), (b) day length, (c) *T* (temperature), and (d) radiation (net radiation). Red, green, and blue points refer to Mediterranean, temperate, and tropical species, respectively. Regression lines across geographical origins are included only when significant differences were found (i.e., in (b) for day length) [Colour figure can be viewed at wileyonlinelibrary.com]

TABLE 1 Effect sizes of the main variables considered as important drivers of stomatal conductance (g_s) of the study *Quercus* species (see also Figure 3)

	VPD	Day length	Temperature	Radiation
Intercept	364.28	−230	88	5.72
Slope	−0.49	28	2.7	0.0014
F or *t* value	−9.4	117.3	6.02	5.95
df	264	264	264	264
P value	<.0001	<.0001	.02	<.0001
R^2	.28	.31	.02	.14

TABLE 2 Results from linear mixed model selection (R^2 = .53) including the significant variables affecting in g_s

Variables	*df*	*F* value	*P* value
Intercept	244	2,142.38	<.0001
Origin	9	5.91	.02
Day length	244	223.1	<.0001
VPD	244	62.31	<.0001
Origin × day length	244	5.22	.006

pressure deficit. Our results thus point to the need of further research to fully understand the underlying mechanisms as well as to explore the necessity of including day-length regulations of stomatal conductance in large-scale modelling and global change studies.

4.1 | Day length regulation of stomatal conductance in *Quercus* spp.

We observed that day length variation affected the seasonality of stomatal conductance across 12 *Quercus* species originating from tropical, Mediterranean, and temperate environments. Furthermore, we observed that the range of variation in g_s driven by the photoperiod (~80 to 200 mmol m^{-2} s^{-1}) was within the range of conductance that limits transpiration (Figure S2). The strongest influence of photoperiod on stomatal conductance was observed in Mediterranean species, which was significantly higher than for tropical and temperate species. Perhaps the simplest explanation for this phenomenon is that Mediterranean oaks experienced the same photoperiod as that occurring in their natural distribution range. Our plants grew at the study site, so they were already acclimated to the photoperiod and thermal regime of this site prior by the time

TABLE 3 Results of model comparison (measured vs. observed) over the *Quercus* dataset obtained in the present study and those for angiosperm and conifer tree data available from the literature

Dataset	Model	AIC	R^2	Intercept	Slope
Quercus spp (this study)	Equation (1) (no photoperiod)	−367.6	.36	−0.01 (0.02)	1.10 (0.13)
	Equation (2) (photoperiod affects the slope)	−414.1	.58	−0.03 (0.01)*	1.22 (0.09)*
	Equation (3) (photoperiod affects the intercept)	−426.2	.52	−0.01 (0.01)	1.08 (0.09)
	Equation (4) (photoperiod affects the slope and intercept)	−424.3	.53	−0-01 (0.01)	1.10 (0.09)*
Angiosperms (literature)	Equation (1) (no photoperiod)	−192.9	.58	−0.003 (0.02)	1.01 (0.11)
	Equation (2) (photoperiod affects the slope)	−197.6	.62	−0.002 (0.02)	1.01 (0.10)
	Equation (3) (photoperiod affects the intercept)	−199.4	.63	−0.003 (0.02)	1.01 (0.10)
	Equation (4) (photoperiod affects the slope and intercept)	−197.7	.63	−0.003 (0.02)	1.01 (0.10)
Conifers (literature)	Equation (1) (no photoperiod)	−272.3	.74	0.00 (0.01)	0.99 (0.08)
	Equation (2) (photoperiod affects the slope)	−275.3	.76	0.00 (0.01)	1.00 (0.07)
	Equation (3) (photoperiod affects the intercept)	−270.7	.74	0.00 (0.01)	1.00 (0.01)
	Equation (4) (photoperiod affects the slope and intercept)	−282.1	.79	0.00 (0.01)	0.99 (0.06)

Note. Values in brackets under intercept and slope indicate the standard error, and the stars indicate that the intercept or slope are significantly different from 1 or 0, respectively, at $P < .05$.

Abbreviation: AIC, Akaike information criterion.

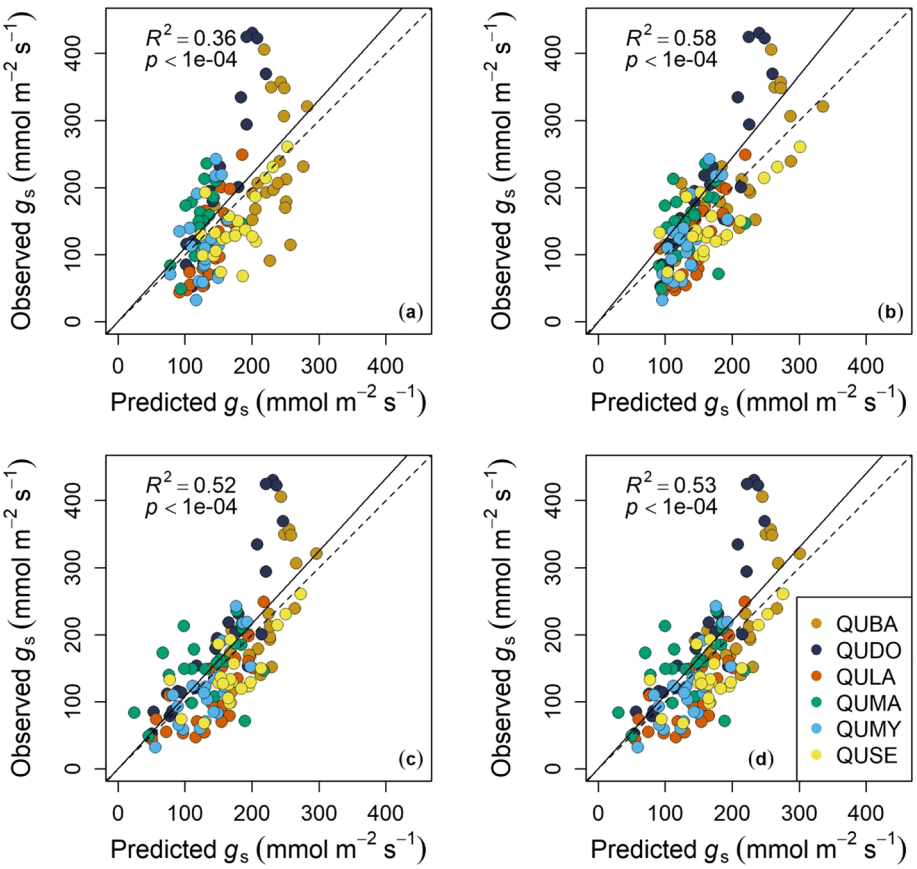

FIGURE 4 Plot of observed versus predicted g_s from the original model of g_s (Equation 1, a) and the modified model version including photoperiod affecting the slope (Equation 2, b), the intercept (Equation 3, c), and the slope and intercept (Equation 4, d). Half of our study species were used for calibration and the other half for validation (only species for validation are shown). The R^2 of the regression of observed versus predicted values and *P* values are given in each panel. Species abbreviations are QUBA (*Quercus ilex* subsp. *ballota*), QUDO (*Quercus douglassi*), QULA (*Quercus lanata*), QUMA (*Quercus macrocarpa*), QUMY (*Quercus myrsinifolia*), and QUSE (*Quercus semecarpifolia*) [Colour figure can be viewed at wileyonlinelibrary.com]

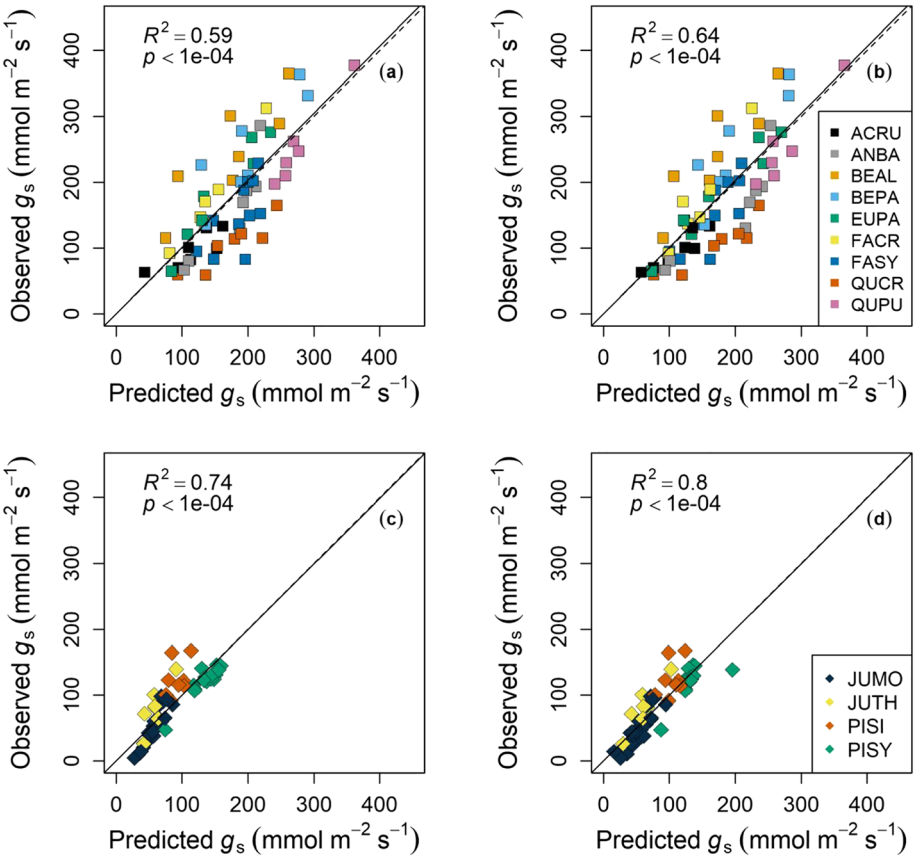

FIGURE 5 Plot of observed versus predicted g_s for hardwood (a, b) and conifer (c, d) species from the literature (Anderegg et al., 2018; Lin et al., 2015; Table S3). For hardwoods, we compare the original model of g_s (Equation 1, a) and the modified model version including photoperiod affecting the intercept (Equation 3, b), and for conifers, we compare the original model of g_s (Equation 1, c) and the modified model version including photoperiod affecting the slope and intercept (Equation 4, d). The R^2 of the regression of observed versus predicted values and P values are given in each panel. Species abbreviations are ACRU (*Acer rubrum*), ANBA (*Angophora bakeri*), BEAL (*Betula alleghaniensis*), BEPA (*Betula papyrifera*), EUPA (*Eucalyptus parramattensis*), FACR (*Fagus crenata*), FASY (*Fagus sylvatica*), QUCR (*Quercus crispula*), QUPU (*Quercus pubescens*), JUMO (*Juniperus monosperma*), JUTH (*Juniperus thurifera*), PISI (*Picea sitchensis*), and PISY (*Pinus sylvestris*) [Colour figure can be viewed at wileyonlinelibrary.com]

of conducting the study. However, Mediterranean plants are likely to be better adapted to Mediterranean photoperiods and thermal regimes than tropical or temperate species. It is thus noteworthy that we also observed significant day-length effects over the seasonal pattern of g_s in temperate and tropical species that were growing outside of their natural range and that experienced a photoperiod markedly different to that in their place of origin.

The sensitivity to day length for Mediterranean trees could be a mechanism of protection against the risks associated with summer stress. That is, Mediterranean springs are often wet and followed by long, protracted droughts. Consequently, timing maximal yearly stomatal conductance in order to coincide with the summer solstice would be especially beneficial for these species so as to maximize carbon gain during the "wet" part of the growing season, before the summer drought kicks in. Although it is known that maximal g_s often occurs early in the season (Rhizopoulou & Mitrakos, 1990), we are the first to show that this seasonal pattern is, at least partly, due to day length control.

4.2 | Can these results be extrapolated to other woody species?

The results from our common garden experiment are limited by the use of a single genus (*Quercus*) and also by the lack of variation in soil water content, which restricts the degree of generalization to be drawn. However, we demonstrated that incorporating day-length regulation into a stomatal conductance model improved the goodness-of-fit across 13 additional angiosperm and gymnosperm trees for which data were available in the literature. Consequently, the observed pattern seems to be general across woody species, and research on day-length stomatal regulation should be at the forefront of our research efforts.

It is well known that vapour pressure deficit exerts a dominant control over the seasonal patterns of stomatal conductance (Damour, Simonneau, Cochard, & Urban, 2010). One of the key challenges for stomatal modelling lies in correctly predicting responses to water stress (Anderegg et al., 2018). Recently, Anderegg et al. (2018) showed

that including stomatal sensitivity to declining water potential in stomatal conductance models increased the predictive capability of previous empirical models under drought conditions. Here, we suggest that incorporating day length may further improve the ability of these models to simulate g_s patterns under drought.

In particular, our analysis indicates that day-length regulation may be particularly important as affecting minimal conductance (g_0). There has been a large body of literature trying to understand the meaning of this parameter (see review by Duursma et al., 2019), as well as its drivers, and here we show, for the first time to our knowledge, that it could vary seasonally with photoperiod. Our results also hint that, in conifers, day-length responses could mediate the slope of stomatal models (g_1), but the generality of this claim remains to be tested because in the available dataset from the literature, there were only four conifer species.

Furthermore, assessments of whether stomata are indeed sensitive to photoperiod using phenomenological models that depend on carbon assimilation (A) should be made with caution. Previous studies have reported that A varies seasonally as a function of photoperiod (Bauerle et al., 2012; Bongers et al., 2017; Stinziano & Way, 2017; Stoy et al., 2014; Way et al., 2017). Therefore, if the photoperiod affects one of our model inputs (e.g., A), then one will very likely also observe that the model output, g_s, is also affected by the photoperiod. Here, we were able to circumvent this problem, at least partly, because we observed that A did not vary seasonally and that it was independent from the photoperiod in our oak species (Figure S1). Also, as we argue in the next manuscript section (see Section 4.3), the most likely mechanism driving photoperiodic stomatal regulation is independent from photoperiodic regulation in A. We thus expect photoperiod regulation in g_s to be independent from photoperiod regulation in A.

Solving the problem of inferring how general and important is photoperiod regulation using a stomatal model that uses a photoperiod-dependent variable as model input requires measurements at high temporal frequency (i.e., weekly or biweekly) such that A and g_s trends may be independently addressed as in our oak study. Unfortunately, the available data that we could compile from the current literature are available only at much coarser temporal frequency (i.e., monthly), preventing a detailed analysis on potential effects of photoperiod regulation in A affecting modelled g_s estimates. Thus, although our study likely provides the most advanced study on the topic to date, additional data collected at higher temporal frequency over a growing season, along with experimental manipulations, will be required to more broadly assess the generality of our findings in species other than *Quercus*.

4.3 | Photoperiodic effect on stomatal conductance: Possible mechanism

One could argue that the higher solar radiation under longer day lengths might be responsible for the higher stomatal conductance. For example, greater g_s could be the result of higher water condensation on the epidermis, which is controlled by radiation (Pieruschka, Huber, & Berry, 2010). Other studies have reported higher leaf hydraulic conductance in response to illumination, which could enhance water delivery close to guard cells favouring stomatal opening (e.g., Scoffoni, Pou, Aasamaa, & Sack, 2008). However, the relationship between g_s and net radiation in our study was significantly weaker than with day length indicating that, although radiation might play a role in regulating seasonal variation in g_s, it cannot fully explain the day length dependence.

Our results of stomatal conductance being regulated by day length might be explained by the circadian clock of guard cells and their interaction with phenology regulatory modules (Hassidim et al., 2017). In blue light, the guard cell plasma membrane H^+-ATPase is activated by the floral integrator FLOWERING LOCUS T (FT), leading to H^+ efflux. The hyperpolarization of the plasma membrane allows K^+ entrance to the guard cell, which induces increased turgor pressure through the water uptake, causing the stomata to open (see Chen, Xiao, Li, & Ni, 2012; Kinoshita et al., 2011, and references therein). The level of FT transcript shows a circadian rhythm, and it is up-regulated by GI (GIGANTEA) and CO (CONSTANS) and repressed by the clock gene ELF3 (EARLY FLORWERING 3) resulting in stomatal closure. Hassidim et al. (2017) showed that the CO/FT regulatory module, component of the photoperiod pathway that regulates flowering time, also controls stomatal aperture in a day-length-dependent manner. The latter study was conducted in *Arabidopsis* plants, but the role of the FT module in the development and phenology has also been reported in trees (Borchert et al., 2015; Hsu et al., 2011; Srinivasan, Dardick, Callahan, & Scorza, 2012). These results suggest that stomatal opening of tree species is likely FT controlled. However, further research is needed to confirm the stomatal regulation of this module together with the functional understanding of such relationships.

Day-length stomatal regulation could serve as a means towards achieving optimal stomatal conductance. Generally speaking, long photoperiods are considered as indicators of "time to grow" and declining photoperiods as indicators of "time to prepare for winter" (Körner et al., 2016). High stomatal conductance during the peak of day length could thus serve to maximize carbon capture during the part of the year when conditions are more favourable towards carbon assimilation. Conversely, the capacity of stomata to use shorter day lengths as indicators of the proximity of the end of the growing season could serve to diminish water use at the time of the year when it would be less efficient.

ACKNOWLEDGMENTS

We acknowledge the support from the talent funds of Southwest University of Science and Technology (18ZX7131) and the Velux Foundation, Switzerland (Project No. 1119; PHOTOCHAIN). We are very grateful to Carlota Oliván and Shengnan Ouyang for their aid in conducting measurements. We sincerely appreciate all valuable comments and suggestions made by the associate editor D. Way and two anonymous referees, which contributed to improve the quality of the article.

AUTHOR CONTRIBUTIONS

V.R.d.D. and E.G. conceived the project. E.G. and A.G. conducted the measurements. E.G.-P., J.J.P.-P., and D.S.-K. cultivated the plants. E.G. and V.R.d.D. analysed the data. E.G. and V.R.d.D. wrote the manuscript. F.B., A.G., E.G.-P., J.J.P.-P., D.S.-K., and N.E.Z. provided useful discussion and insights into the analysis and discussion. All co-authors contributed to the edits of the manuscript.

FUNDING INFORMATION

The present study has been supported from the talent funds of Southwest University of Science and Technology (18ZX7131) and the Velux Foundation, Switzerland (Project No. 1119; PHOTOCHAIN).

DATA ACCESSIBILITY STATEMENT

The data presented in the paper are available via the TRY data repository (Kattge et al., 2020)

ORCID

Elena Granda https://orcid.org/0000-0002-9559-4213
Frederik Baumgarten https://orcid.org/0000-0002-8284-8384
Arthur Gessler https://orcid.org/0000-0002-1910-9589
Eustaquio Gil-Pelegrin https://orcid.org/0000-0002-4053-6681
Jose Javier Peguero-Pina https://orcid.org/0000-0002-8903-2935
Domingo Sancho-Knapik https://orcid.org/0000-0001-9584-7471
Niklaus E. Zimmerman https://orcid.org/0000-0003-3099-9604
Víctor Resco de Dios https://orcid.org/0000-0002-5721-1656

REFERENCES

Anderegg, W. R. L., Wolf, A., Arango-Velez, A., Choat, B., Chmura, D. J., Jansen, S., … Pacala, S. (2018). Woody plants optimise stomatal behaviour relative to hydraulic risk. *Ecology Letters*, *21*, 968–977. https://doi.org/10.1111/ele.12962

Ball, J. T., Woodrow, I. E., & Berry, J. A. (1987). A model predicting stomatal conductance and its contribution to the control of photosynthesis under different environmental conditions. *Progress in Photosynthesis Research*, *IV*, 221–224.

Barton K. (2018) MuMIn: Multi-model inference.

Basler, D., & Körner, C. (2012). Photoperiod sensitivity of bud burst in 14 temperate forest tree species. *Agricultural and Forest Meteorology*, *165*, 73–81.

Bates, D. M., & Watts, D. G. (1988). *Nonlinear regression analysis and its applications*. New York: Wiley.

Bauerle, W. L., Oren, R., Way, D. A., Qian, S. S., Stoy, P. C., Thornton, P. E., … Reynolds, R. F. (2012). Photoperiodic regulation of the seasonal pattern of photosynthetic capacity and the implications for carbon cycling. *Proceedings of the National Academy of Sciences*, *109*, 8612–8617. https://doi.org/10.1073/pnas.1119131109

Becklin, K. M., Anderson, J. T., Gerhart, L. M., Wadgymar, S. M., Wessinger, C. A., & Ward, J. K. (2016). Examining plant physiological responses to climate change through an evolutionary lens. *Plant Physiology*, *172*, 635–649. https://doi.org/10.1104/pp.16.00793

Bongers, F. J., Olmo, M., Lopez-Iglesias, B., Anten, N. P., & Villar, R. (2017). Drought responses, phenotypic plasticity and survival of Mediterranean species in two different microclimatic sites. *Plant Biology (Stuttgart, Germany)*, *19*, 386–395. https://doi.org/10.1111/plb.12544

Borchert, R., Calle, Z., Strahler, A. H., Baertschi, A., Magill, R. E., Broadhead, J. S., … Muthuri, C. (2015). Insolation and photoperiodic control of tree development near the equator. *New Phytologist*, *205*, 7–13. https://doi.org/10.1111/nph.12981

Burnham, K. P., & Anderson, D. R. (2002). *Model Selection and Multi/Model Inference: A Practical Information-Theoretic Approach*. New York: Springer-;Verlag.

Chen, C., Xiao, Y. G., Li, X., & Ni, M. (2012). Light-regulated stomatal aperture in *Arabidopsis*. *Molecular Plant*, *5*, 566–572.

Curtis, C. J., & Simpson, G. L. (2014). Trends in bulk deposition of acidity in the UK, 1988–2007, assessed using additive models. *Ecological Indicators*, *37*, 274–286. https://doi.org/10.1016/j.ecolind.2012.10.023

Damour, G., Simonneau, T., Cochard, H., & Urban, L. (2010). An overview of models of stomatal conductance at the leaf level. *Plant, Cell and Environment*, *33*, 1419–1438.

Duursma, R. A., Blackman, C. J., Lopéz, R., Martin-StPaul, N. K., Cochard, H., & Medlyn, B. E. (2019). On the minimum leaf conductance: Its role in models of plant water use, and ecological and environmental controls. *New Phytologist*, *221*, 693–705. https://doi.org/10.1111/nph.15395

Gil-Pelegrín E., Peguero-Pina J.J. & Sancho-Knapik D. (2017) *Oaks physiological ecology. Exploring the functional diversity of genus* Quercus *L.*

Hagedor n, F., Joseph, J., Peter, M., Luster, J., Pritsch, K., Geppert, U., … Arend, M. (2016). Recovery of trees from drought depends on belowground sink control. *Nature Plants*, *2*, 16111. https://doi.org/10.1038/nplants.2016.111

Hassidim, M., Dakhiya, Y., Turjeman, A., Hussien, D., Shor, E., Anidjar, A., … Green, R. M. (2017). CIRCADIAN CLOCK ASSOCIATED 1 (CCA1) and the circadian control of stomatal aperture. *Plant Physiology*, *175*, 01214. 2017

Hastie, T. J., & Tibshirani, R. J. (1990). *Generalized additive models, volume 43 of monographs on statistics and applied probability*. London: Chapman & Hall.

Hsu, C.-Y., Adams, J. P., Kim, H., No, K., Ma, C., Strauss, S. H., … Yuceer, C. (2011). FLOWERING LOCUS T duplication coordinates reproductive and vegetative growth in perennial poplar. *Proceedings of the National Academy of Sciences*, *108*, 10756–10761. https://doi.org/10.1073/pnas.1104713108

Jackson, S. D. (2009). Plant responses to photoperiod. *New Phytologist*, *181*, 517–531. https://doi.org/10.1111/j.1469-8137.2008.02681.x

Kattge J., Bönisch G., Díaz S., Lavorel S., Prentice I.C., Leadley P., . . . Wirth C. (2020). TRY plant trait database —enhanced coverage and open access. *Global Change Biology*.

Kinoshita, T., Ono, N., Hayashi, Y., Morimoto, S., Nakamura, S., Soda, M., … Shimazaki, K. I. (2011). FLOWERING LOCUS T regulates stomatal opening. *Current Biology*, *21*, 1232–1238. https://doi.org/10.1016/j.cub.2011.06.025

Körner, C., Basler, D., Hoch, G., Kollas, C., Lenz, A., Randin, C. F., … Zimmermann, N. E. (2016). Where, why and how? Explaining the low-temperature range limits of temperate tree species. *Journal of Ecology*, *104*, 1076–1088. https://doi.org/10.1111/1365-2745.12574

Leuning, R. (1995). A critical appraisal of a combined stomatal-photosynthesis model for C_3 plants. *Plant, Cell & Environment*, *18*, 339–355. https://doi.org/10.1111/j.1365-3040.1995.tb00370.x

Lin, Y. S., Medlyn, B. E., Duursma, R. A., Prentice, I. C., Wang, H., Baig, S., … Wingate, L. (2015). Optimal stomatal behaviour around the world.

Nature Climate Change, *5*, 459–464. https://doi.org/10.1038/nclimate2550

Luo, T., Liu, X., Zhang, L., Li, X., Pan, Y., & Wright, I. J. (2018). Summer solstice marks a seasonal shift in temperature sensitivity of stem growth and nitrogen-use efficiency in cold-limited forests. *Agricultural and Forest Meteorology*, *248*, 469–478. https://doi.org/10.1016/j.agrformet.2017.10.029

Medlyn, B. E., Duursma, R. A., Eamus, D., Ellsworth, D. S., Prentice, I. C., Barton, C. V. M., … Wingate, L. (2011). Reconciling the optimal and empirical approaches to modelling stomatal conductance. *Global Change Biology*, *17*, 2134–2144. https://doi.org/10.1111/j.1365-2486.2010.02375.x

Nakagawa, S., & Schielzeth, H. (2013). A general and simple method for obtaining R^2 from generalized linear mixed-effects models. *Methods in Ecology and Evolution*, *4*, 133–142. https://doi.org/10.1111/j.2041-210x.2012.00261.x

Pieruschka, R., Huber, G., & Berry, J. A. (2010). Control of transpiration by radiation. *Proceedings of the National Academy of Sciences*, *107*, 13372–13377. https://doi.org/10.1073/pnas.0913177107

Pinheiro, J, Bates, D, DebRoy, S, Sarkar, D. R. C. T. (2018) nlme: Linear and nonlinear mixed effects models. R package version 3.1-137, https://CRAN.R-project.org/package=nlme. R Package Version 3.1–137, *https://CRAN.R-project.org/package=nlme*.

R Development Core Team (2018). *R: A language and environment for statistical computing*. Vienna, Austria: R Foundation for Statistical Computing. Retrieved from http://www.R-project.org/

Resco de Dios, V., & Gessler, A. (2018). Circadian regulation of photosynthesis and transpiration from genes to ecosystems. *Environmental and Experimental Botany*, *152*, 37–48. https://doi.org/10.1016/j.envexpbot.2017.09.010

Rhizopoulou, S., & Mitrakos, K. (1990). Water relations of evergreen sclerophylls. I. Seasonal changes in the water relations of eleven species from the same environment. *Annals of Botany*, *65*, 171–178. https://doi.org/10.1093/oxfordjournals.aob.a087921

Rossi, S., Deslauriers, A., Anfodillo, T., Morin, H., Saracino, A., Motta, R., & Borghetti, M. (2006). Conifers in cold environments synchronize maximum growth rate of tree-ring formation with day length. *The New Phytologist*, *170*, 301–310. https://doi.org/10.1111/j.1469-8137.2006.01660.x

Saikkonen, K., Taulavuori, K., Hyvönen, T., Gundel, P. E., Hamilton, C. E., Vänninen, I., … Helander, M. (2012). Climate change-driven species' range shifts filtered by photoperiodism. *Nature Climate Change*, *2*, 239–242. https://doi.org/10.1038/nclimate1430

Scoffoni, C., Pou, A., Aasamaa, K., & Sack, L. (2008). The rapid light response of leaf hydraulic conductance: New evidence from two experimental methods. *Plant, Cell and Environment*, *31*, 1803–1812. https://doi.org/10.1111/j.1365-3040.2008.01884.x

Srinivasan, C., Dardick, C., Callahan, A., & Scorza, R. (2012). Plum (*Prunus domestica*) trees transformed with poplar FT1 result in altered architecture, dormancy requirement, and continuous flowering. *PLoS ONE*, *7*, e40715. https://doi.org/10.1371/journal.pone.0040715

Stinziano, J. R., & Way, D. A. (2017). Autumn photosynthetic decline and growth cessation in seedlings of white spruce are decoupled under warming and photoperiod manipulations. *Plant, Cell and Environment*, *40*, 1296–1316. https://doi.org/10.1111/pce.12917

Stoy, P. C., Trowbridge, A. M., & Bauerle, W. L. (2014). Controls on seasonal patterns of maximum ecosystem carbon uptake and canopy-scale photosynthetic light response: Contributions from both temperature and photoperiod. *Photosynthesis Research*, *119*, 49–64. https://doi.org/10.1007/s11120-013-9799-0

Tylewicz, S., Petterle, A., Marttila, S., Miskolczi, P., Azeez, A., Singh, R. K., … Bhalerao, R. P. (2018). Photoperiodic control of seasonal growth is mediated by ABA acting on cell–cell communication. *Science*, *360*, 212–215. https://doi.org/10.1126/science.aan8576

Way, D. A., & Montgomery, R. A. (2015). Photoperiod constraints on tree phenology, performance and migration in a warming world. *Plant, Cell and Environment*, *38*, 1725–1736. https://doi.org/10.1111/pce.12431

Way, D. A., Stinziano, J. R., Berghoff, H., & Oren, R. (2017). How well do growing season dynamics of photosynthetic capacity correlate with leaf biochemistry and climate fluctuations? *Tree Physiology*, *37*, 879–888. https://doi.org/10.1093/treephys/tpx086

Wood S.N. (2017) Generalized additive models: An introduction with R, second edition.

Zhao, H., Li, Y., Duan, B., Korpelainen, H., & Li, C. (2009). Sex-related adaptive responses of *Populus cathayana* to photoperiod transitions. *Plant, Cell and Environment*, *32*, 1401–1411. https://doi.org/10.1111/j.1365-3040.2009.02007.x

Zohner, C. M., Benito, B. M., Svenning, J. C., & Renner, S. S. (2016). Day length unlikely to constrain climate-driven shifts in leaf-out times of northern woody plants. *Nature Climate Change*, *6*, 1120–1123. https://doi.org/10.1038/nclimate3138

Zohner, C. M., & Renner, S. S. (2015). Perception of photoperiod in individual buds of mature trees regulates leaf-out. *New Phytologist*, *208*, 1023–1030. https://doi.org/10.1111/nph.13510

SUPPORTING INFORMATION

Additional supporting information may be found online in the Supporting Information section at the end of the article.

Table S1. Study species, separated by three different geographical domains (TRO, tropical; MED, Mediterranean and TEM, temperate) according to the latitudinal range of their actual distribution. Listed are also leaf type (D, deciduous; E, evergreen), altitudinal range (m a.s.l.), minimum, maximum and mean latitudes (°), and geographical distribution of the selected species.

Table S2. AIC values for the different models tested, showing that Medlyn's model provided slightly lower AIC.

Table S3. Species for which data was available from the literature (Anderegg et al., 2018; Lin et al., 2015). Listed are also functional type (temperate deciduous, temperate evergreen, boreal conifer, temperate conifer), location, latitude, longitude, mean annual temperature (1980–2014, (MAT) and mean annual precipitation (MAP) for the sites where the measurements were conducted (Harris, Jones, Osborn, & Lister, 2014), and the correspondent reference.

Figure S1. Temporal patterns obtained fitting generalized additive models of photosynthesis at saturating light (A_{sat}) of the a) temperate (TEM), b) Mediterranean (MED) and c) tropical (TRO) species since the beginning of June until the end of October. We computed the first derivative to test whether the trend was significantly positive or negative (see methods), and the yellow parts of the curve indicate significant increasing or decreasing slopes. There is no significant seasonal variation in *A* for TEM and MED species and there is no significant decline after July in TRO. Since this pattern of variation is different than that from g_s, it can be inferred that the seasonal variation in g_s

does not result from seasonal variation in *A*. Panel d) shows the linear relationship between A_{sat} and day-length as in Figure 3.

Figure S2. Relationship between stomatal conductance (g_s) and transpiration (E) for the study *Quercus* species during weekly measurements along the growing season.

How to cite this article: Granda E, Baumgarten F, Gessler A, et al. Day length regulates seasonal patterns of stomatal conductance in *Quercus* species. *Plant Cell Environ*. 2020;43: 28–39. https://doi.org/10.1111/pce.13665